

MH₂P₂O₇ (M = Co, Ni): Metamagnetic Interaction between the Zigzag Octahedral Chains

Tao Yang,[†] Jing Ju,[‡] Guobao Li,[†] Sihai Yang,[†] Junliang Sun,[†] Fuhui Liao,[†] Jianhua Lin,^{*,†} Juns Sasaki,[‡] and Naoki Toyota[‡]

Beijing National Laboratory for Molecular Sciences, State Key Laboratory for Rare Earth Materials Chemistry and Applications, College of Chemistry and Molecular Engineering, Peking University, Beijing 100871, People's Republic of China, and Physics Department, Graduate School of Science, Tohoku University, Sendai 980-8578, Japan

Received September 3, 2006

CoH₂P₂O₇ and NiH₂P₂O₇, which contain edge-sharing zigzag octahedral chains, were hydrothermally synthesized and structurally characterized. Both compounds exhibit field-induced metamagnetic behavior because of the strong intrachain ferromagnetic and relatively weak interchain antiferromagnetic interactions.

An extraordinarily large number of phosphates have been characterized during the past 2 decades, initiated by the discovery of the vast structural variety in aluminum phosphates¹ (1982) and zinc phosphates² (1991). Phosphates containing transition metals are particularly interesting because of their potential applications as cathodes for lithium batteries,³ proton conductors,⁴ and heterogeneous catalysts.⁵ On the other hand, the complex structures of the transition-metal phosphates have also been used to trace the magnetic interaction of transition-metal ions. In many cases, iron,⁶ manganese,⁷ cobalt,⁸ nickel,^{8b,9} and chromium ions¹⁰ are octahedrally coordinated in phosphates and could form an

oligomer, a chain, or a layer via corner- or edge-sharing. The interaction between the transition-metal ions may lead to metamagnetic behavior under certain conditions, such as a field-induced antiferromagnetic (AF) to ferromagnetic (FM) transition in MIL-38^{6c} and field-induced spin flip in SrFe₂(PO₄)₂.^{6f} Here we report two new transition-metal phosphates, CoH₂P₂O₇ (**1**) and NiH₂P₂O₇ (**2**). The intra- and interchain magnetic interactions lead to interesting field-induced effects in these compounds.

1 and **2** (MH₂P₂O₇; M = Co, Ni)¹¹ are isostructural, crystallizing in *P*2₁/*c*, as shown in Table 1. An asymmetric unit contains 2 M, 4 P, and 14 O, all located in the general positions. The transition-metal ions are octahedrally coordinated by O atoms, which share two edges, forming a zigzag chain. The P atoms are tetrahedrally coordinated in a polyphosphate P₂O₇ group, which further shares corners with the octahedra via two kinds of 3-rings, i.e., the 3-ring of two octahedra and one tetrahedron and of one octahedron and two tetrahedra (Figure 1a). The bond distances and angles in **1** and **2** are all regular, as in other known phosphates. For example, bond distances and angles in **1** range from 1.973(3) to 2.166(3) Å and from 77.80(11) to 99.49(11)° for the CoO₆ octahedron and from 1.485(3) to

* To whom correspondence should be addressed. E-mail: jhlin@pku.edu.cn. Fax: 8610-62751708.

[†] Peking University.

[‡] Tohoku University.

- (1) Wilson, S. T.; Loc, B. M.; Messina, C. A.; Cannan, T. R.; Flanigen, E. M. *J. Am. Chem. Soc.* **1982**, *104*, 1146–1147.
- (2) Gier, T. E.; Stucky, G. D. *Nature (London)* **1991**, *349*, 508–510.
- (3) (a) Alvarez-Vega, M.; Garcia-Moreno, O.; Garcia-Alvarado, F.; Garcia-Jaca, J.; Gallardo-Amores, J. M.; Sanjuan, M. L.; Amador, U. *Chem. Mater.* **2001**, *13*, 1570–1576. (b) Yang, S.; Zavalij, P. Y.; Whittingham, M. S. *Electrochem. Commun.* **2001**, *3*, 505–508.
- (4) Alberti, G.; Casciola, M.; Costantino, U.; Vivani, R. *Adv. Mater.* **1996**, *8*, 291–303.
- (5) (a) Millet, J. M. M. *Catal. Rev.* **1998**, *40*, 1–38. (b) Bonnet, P.; Millet, J. M. M.; Leclercq, C.; Vadrine, J. C. *J. Catal.* **1996**, *158*, 128–141.
- (6) (a) Riou-Cavellev, M.; Riou, D.; Férey, G. *Inorg. Chim. Acta* **1999**, *291*, 317–325. (b) Goñi, A.; Lezama, L.; Espina, A.; Trobajo, C.; García, J. R.; Rojo, T. *J. Mater. Chem.* **2001**, *11*, 2315–2319. (c) Song, Y.; Zavalij, P. Y.; Suzuki, M.; Whittingham, M. S. *Inorg. Chem.* **2002**, *41*, 5778–5786. (d) Fernández, S.; Mesa, J. L.; Pizarro, J. L.; Lezama, L.; Arriortua, M. I.; Rojo, T. *Chem. Mater.* **2002**, *14*, 2300–2307. (e) Riou-Cavellev, M.; Sanselme, M.; Noguès, M.; Grenèche, J. M.; Férey, G. *Solid State Sci.* **2002**, *4*, 619–625. (f) Belik, A. A.; Azuma, M.; Takano, M.; Lazoryak, B. I. *Chem. Mater.* **2004**, *16*, 4311–4318. (g) Mandal, S.; Pati, S. K.; Green, M. A.; Natarajan, S. *Chem. Mater.* **2005**, *17*, 2912–2917.
- (7) (a) Wright, A. J.; Attfiel, J. P. *Inorg. Chem.* **1998**, *37*, 3858–3861. (b) Wright, A. J.; Attfiel, J. P. *J. Solid State Chem.* **1998**, *141*, 160–163. (c) Escobal, J.; Pizarro, J. L.; Mesa, J. L.; Lezama, L.; Olazcuaga, R.; Arriortua, M. I.; Rojo, T. *Chem. Mater.* **2000**, *12*, 376–382. (d) Lethbride, Z. A. D.; Hillier, A. D.; Cywinski, R.; Lightfoot, P. *J. Chem. Soc., Dalton Trans.* **2000**, 1595–1599. (e) Song, Y.; Zavalij, P. Z.; Chernova, N. A.; Whittingham, M. S. *Chem. Mater.* **2003**, *15*, 4968–4973.
- (8) (a) Chen, J.; Jones, R. H.; Natarajan, S.; Hursthouse, M. B.; Thomas, J. M. *Angew. Chem., Int. Ed. Engl.* **1994**, *33*, 639–640. (b) Humanaka, N.; Imoto, H. *Inorg. Chem.* **1998**, *37*, 5884–5885. (c) Chang, W. K.; Chiang, R. K.; Jiang, Y. C.; Wang, S. L.; Lee, S. F.; Lii, K. H. *Inorg. Chem.* **2004**, *43*, 2564–2568. (d) Mandal, S.; Natarajan, S. *J. Solid State Chem.* **2005**, *178*, 2376–2382. (e) Belik, A. A.; Azuma, M.; Takano, M. *Inorg. Chem.* **2005**, *44*, 7523–7529.
- (9) Cuillou, N.; Gao, Q.; Forster, P. M.; Chang, J. S.; Noguès, M.; Park, S. E.; Férey, G.; Cheetham, A. K. *Angew. Chem., Int. Ed.* **2001**, *40*, 2831–2834.
- (10) Fernández, S.; Mesa, J. L.; Pizarro, J. L.; Lezama, L.; Arriortua, M. I.; Rojo, T. *Angew. Chem., Int. Ed.* **2002**, *41*, 3683–3685.

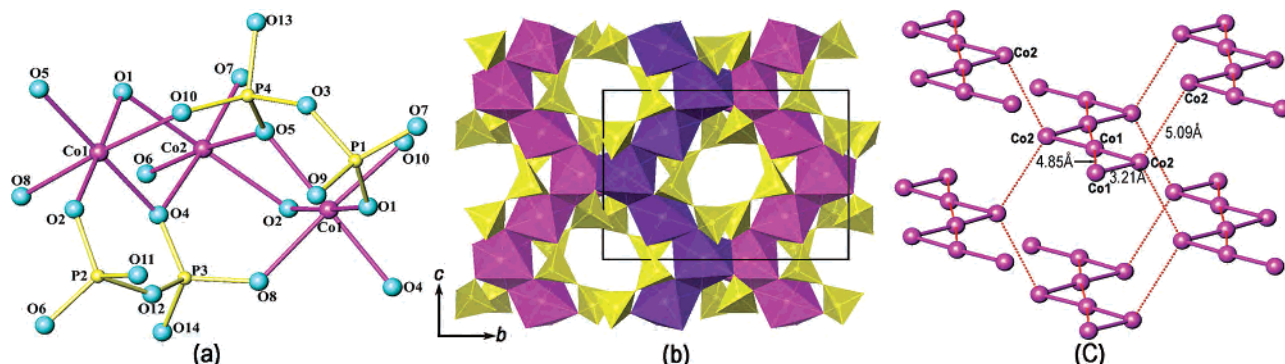


Figure 1. (a) Structure fragment of $\text{CoH}_2\text{P}_2\text{O}_7$. (b) Projection view along the a axis. All of the H atoms are omitted for clarity. (c) Transition-metal ion backbone of **1**. A stick line represents the distance between Co1–Co2 in 3.14 Å. Dotted lines represent the distance between Co1–Co1 in 4.85 Å and Co2–Co2 in 5.09 Å.

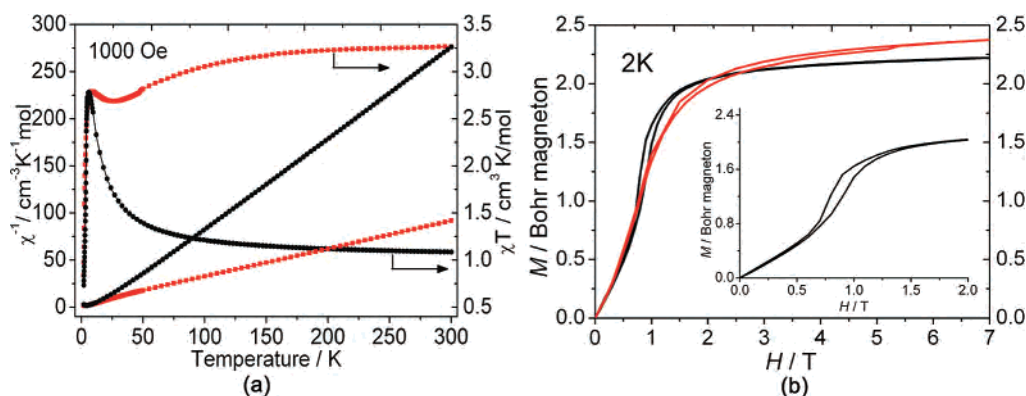


Figure 2. (a) χ_M^{-1} and $\chi_M T$ vs temperature curves of $\text{CoH}_2\text{P}_2\text{O}_7$ (**1**, red) and $\text{NiH}_2\text{P}_2\text{O}_7$ (**2**, black) at 1000 Oe. (b) Magnetization curves of $\text{MH}_2\text{P}_2\text{O}_7$ ($M = \text{Co}, \text{Ni}$) at 2 K. The inset is the amplification of a FM hysteresis loop of $\text{NiH}_2\text{P}_2\text{O}_7$.

Table 1. Crystallographic Parameters for Title Compounds

formula	$\text{CoH}_2\text{P}_2\text{O}_7$	$\text{NiH}_2\text{P}_2\text{O}_7$
fw	234.88	234.67
space group	$P2_1/c$	$P2_1/c$
a (Å)	9.1658(18)	9.0960(18)
b (Å)	12.681(3)	12.593(3)
c (Å)	9.6882(19)	9.5999(19)
β (deg)	106.74(3)	106.47(3)
V (Å ³)	1078.3(4)	1054.5(4)
ρ_{calcd} (g/cm ³)	2.894	2.956
$\mu(\text{Mo K}\alpha)$ (mm ⁻¹)	3.753	4.263
R1	0.0454	0.0320
wR2	0.1665	0.1128

1.605(3) Å and from 98.40(17)° to 115.51(18)° in the P_2O_7 group. The calculated bond valence sums (BVSs) of the metal atoms are all close to 2 [BVS = 2.034 (Co1), 2.022 (Co2), 1.997 (Ni1), and 1.981 (Ni2)]. However, the BVS values of some O positions are significantly lower [O9 (1.1), O11 (1.2), O13 (1.1), and O14 (1.1)], indicative of a possible binding with protons. In IR spectra, two broad bands at about 2915 and 3392 cm^{-1} were observed, originating from the vibration of the OH groups. Dehydration of the hydroxyl groups occurs at about 400 °C, accompanied by a weight loss of about 7.0 wt % (calcd 7.7 wt %).

The MO_6 octahedral zigzag chains are running along the c axis in the structure, as shown in different colors in Figure 1b for clarity, and are further interconnected through P_2O_7 groups, forming a three-dimensional structure. Although the structure is three-dimensional and, in addition, contains small intersectional 10- and 8-ring channels along the a and c axes, respectively, the magnetic interaction of the transition-metal

ions should be one-dimensional as far as the M–M distances are concerned. The shortest M–M distance is 3.21 Å for Co (**1**) and 3.14 Å for Ni (**2**) within the octahedral chain and 5.09 Å for Co and 5.06 Å for Ni between the chains. In Figure 2c, we show the arrangement of the transition-metal atoms in the structure. Interestingly, this zigzag octahedral chain is quite stable, which may persist in the dehydration products of **1** and **2**. The dehydration products of **1** and **2**

(11) Synthesis: 2 mmol of $\text{M}(\text{CH}_3\text{COO})_2 \cdot \text{H}_2\text{O}$ ($M = \text{Co}, \text{Ni}$) and 3 mL of concentrated H_3PO_4 (14.6 mol/L) were charged into a 50-mL Teflon reactor and heated at 220 °C for 4 days. After cooling to room temperature, the solid products were isolated by washing with alcohol or cold water. $\text{CoH}_2\text{P}_2\text{O}_7$ is not stable in hot water. The single crystals are purple for Co and green for Ni. The yield of the product is about 80% according to the transition metal. Other transition-metal resources such as divalent metal chlorides or nitrates are also effectual. Analyses: crystals of $\text{CoH}_2\text{P}_2\text{O}_7$ of about $0.2 \times 0.2 \times 0.3 \text{ mm}^3$ were used for single-crystal data collection at 293 K on a Rigaku AFC6S diffractometer with graphite-monochromated Mo K α radiation ($\lambda = 0.71073 \text{ \AA}$) by the ω - 2θ scan method. The structure was solved by using direct methods and refined on F^2 with full-matrix least-squares methods using *SHELXS-97* and *SHELXL-97* programs.¹⁵ A total of 2005 reflections were measured in $2.32^\circ < \theta < 25.50^\circ$. Magnetic measurements were carried out on a superconducting quantum interference device magnetometer (SQUID, Quantum Design Co.) in the temperature range from 2 to 300 K under an applied field H of 1000 Oe. The magnetization curves were measured at 2 K up to $H = 7 \text{ T}$. Chemical analysis was carried out using an inductively coupled plasma method on an ESCALAB2000 analyzer (Co:P = 1.0:2.1; Ni:P = 1.0:2.0). The thermal stability was analyzed with thermogravimetric analysis (TGA) on a Dupont 951 thermogravimetric analyzer in air with a heating rate of 10 °C/min from 30 to 800 °C. IR spectra (Nicolet Magna-IR-750 series II) confirm the presence of hydroxyl groups.

are the known transition-metal cyclotetraphosphates¹² Ni₂P₄O₁₂ and Co₂P₄O₁₂. Their structures consist of the zigzag octahedral chains, but they are interconnected by [P₄O₁₂]⁴⁻ groups instead of [H₂P₂O₇]²⁻ as in **1** and **2**.

The magnetic susceptibility follows Curie–Weiss law at high temperature with $C = 3.3 \text{ cm}^3 \cdot \text{K/mol}$ and $\theta = -9.4 \text{ K}$ for **1** and $C = 1.1 \text{ cm}^3 \cdot \text{K/mol}$ and $\theta = 10.9 \text{ K}$ for **2**, corresponding to $\mu_{\text{eff}} = 5.1 \mu_{\text{B}}$ and $3.0 \mu_{\text{B}}$, respectively (Figure 2a). The observed effective magnetic moment of **2** agrees with the spin-only Ni²⁺ (d⁸; $\mu_{\text{cal}} = 2.82 \mu_{\text{B}}$ for $S = 1$) system. For the Co system, however, the observed effective moment is higher than the spin-only value (d⁷; $\mu_{\text{cal}} = 3.87 \mu_{\text{B}}$ for $S = 3/2$) owing to the strong spin–orbit coupling in the Co system.¹³

The positive Weiss constant of **2** and an increase of $\chi_{\text{M}}T$ from 40 to 6 K imply a predominant FM interaction within the chains in this temperature range. The sharp decreases in the χT curves below 6 K indicate a long-range AF ordering, and T_{N} is about 4 K estimated from the $d(\chi_{\text{M}}T)/dT$ curve. According to the structure of the metal sublattice (Figure 1c), it is presumed that the FM coupling originates from intrachain Ni²⁺–O–Ni²⁺ interaction, while the low-temperature AF ordering may originate from the antiparallel alignment of these FM chains through Ni₂–O–P–O–Ni₂ interchain superexchange. Additionally, the magnetization plot of **2** exhibits a sigmoidal shape and a large hysteresis loop at a high external field (0.7–1.5 T; Figure 2b). These phenomena are characteristic of metamagnetism, which can also be understood by the above assumption. Under a high external field (>0.90 T) at low temperature, the FM chains switch from mainly an antiparallel setting to mainly a parallel setting, which leads to a FM ordering at a high external field as indicated by the hysteresis loop. The saturation magnetization at 7 T is about $2.2 \mu_{\text{B}}$, slightly larger than the theoretical value of $2 \mu_{\text{B}}$. This compound might be an interesting example in which the metamagnetism originated from the coexistence of strong intrachain FM and relatively weak AF interchain couplings. Comparatively, a similar field-induced magnetic transition was also observed for [Co₃(pyz)-(HPO₄)₂F₂],^{8c} where the magnetic interaction is FM within the layer and AF between the layers.

The magnetic susceptibility ($\chi_{\text{M}}T$) of **1** behaves differently, as shown in Figure 2a. In the high-temperature range (>40 K), the $\chi_{\text{M}}T$ value decreases gradually as the temperature goes down. In addition, the Weiss constant θ has a negative

value (−9.4 K). However, this does not definitely mean the magnetic interaction is AF within the octahedral zigzag chain but is rather due to the single-ion behavior of Co²⁺ ions as observed in some other Co-containing compounds, such as Co[(N(CN)₂)₂(pzdo)] and Co[(N(CN)₂)₂(mpdo)].¹⁴ At low temperature (<28 K), $\chi_{\text{M}}T$ increases and exhibits a maximum at about 7.8 K and then decreases rapidly, indicating an AF ordering below this temperature. The magnetization curve at 2 K shows a behavior similar to that of **2** (Figure 2b). It increases linearly at low field and then shows a narrow magnetic hysteresis at a high external field. According to the present experimental evidence, we would rather assume that the magnetic interaction in **1** is similar to that in **2**. At low temperature, the AF coupling of the FM chains leads to an AF ground state. With an increase in the external magnetic field ($H_{\text{c}} = 0.85 \text{ T}$), the FM chains tend to parallelly align, resulting in FM ordering. However, because of the strong spin–orbit coupling of Co²⁺ ions, the magnetic interaction might be more complicated. This needs to be further studied by other techniques, such as neutron diffraction, etc.

In conclusion, we illustrated that two hydrated transition-metal phosphates, CoH₂P₂O₇ (**1**) and NiH₂P₂O₇ (**2**), exhibit interesting magnetic properties. The structure of these two phosphates contains edge-sharing zigzag octahedral (MO₆) chains, which are interconnected by P₂O₇ groups and thus can be considered as quasi-one-dimensional, in particular, where magnetic interactions are concerned. These two compounds exhibit a field-induced metamagnetic behavior from an AF state to a FM state. The observed metamagnetic property can be understood by assuming strong intrachain FM and weak interchain AF interactions. A high magnetic field may therefore switch the orientation of the magnetic moment of the FM chains, which leads to a primarily FM ordering at a high magnetic field.

Acknowledgment. We thank Prof. Song Gao and Zheming Wang for helpful discussion on magnetism. This work was supported by the Nature Science Foundation of China, under Contract 20221101.

Supporting Information Available: Crystal details in CIF format and IR, TGA, and $d(\chi T)/dT$ and $d(M)/d(H)$ curves. This material is available free of charge via the Internet at <http://pubs.acs.org>.

IC061665Q

(12) Olbertz, A.; Stachel, D.; Svoboda, I.; Fuess, H. Z. *Kristallogr.—New Cryst. Struct.* **1998**, *213*, 241–242.

(13) Cotton, F. A.; Wilkinson, G.; Murillo, C. O.; Bochmann, M.; *Advanced Inorganic Chemistry*; John Wiley & Sons: New York, 1999; Chapter 17.

(14) Sun, H. L.; Gao, S.; Ma, B. Q.; Su, G. *Inorg. Chem.* **2003**, *42*, 5399–5404.

(15) Sheldrick, G. M. *SHELXS 97, Program for the solution of crystal structures*; University of Göttingen: Göttingen, Germany, 1997. Sheldrick, G. M. *SHELXL 97, Program for the refinement of crystal structures*; University of Göttingen: Göttingen, Germany, 1997.